



OPEN

Fused deposition modeling process parameter optimization on the development of graphene enhanced polyethylene terephthalate glycol

S. Raja¹✉, M. Jayalakshmi², Maher Ali Rusho³, Vinoth Kumar Selvaraj⁴,
Jeyanthi Subramanian⁴, Simon Yishak⁵✉ & T. Arun Kumar¹

This study investigates the production of graphene-enhanced polyethylene terephthalate glycol (G-PETG) components using fused deposition modeling (FDM) and evaluates their mechanical properties, contributing to the advancement of additive manufacturing. Trials demonstrated notable improvements in mechanical performance, with optimal printing parameters identified using the Spice Logic Analytical Hierarchy Process (AHP). The effectiveness of this methodology is further compared with the Fuzzy Analytic Hierarchy Process (FAHP) combined with the Technique for Order of Preference by Similarity to Ideal Solution (TOPSIS). The study revealed significant enhancements, with the ultimate tensile strength (UTS) reaching 69.1 MPa, an average Young's modulus of 735.6 MPa, and an ultimate compressive strength (UCS) of 85.3 MPa. These findings provide valuable insights into optimizing techniques for improving the mechanical performance of G-PETG components, advancing material applications in various industries.

Keywords Additive manufacturing, Mechanical properties, Polymer matrix composites, Graphene reinforcement, 3D printing optimization, Industrial applications, Materials science

Additive manufacturing (AM), commonly referred to as 3D printing, has revolutionized the production of complex and customized components, particularly in the field of polymer-based materials. Among the various AM techniques, Fused Deposition Modeling (FDM) has emerged as a leading method for fabricating intricate designs with high precision. FDM offers significant advantages, including material efficiency, reduced waste, and the ability to rapidly prototype components^{1–3}. However, to fully realize the potential of FDM in producing high-performance components, optimizing printing parameters and material properties remains crucial.

One material gaining significant attention in AM is Polyethylene Terephthalate Glycol (PETG), a popular thermoplastic known for its chemical resistance, durability, and ease of printing. When reinforced with graphene, a material renowned for its exceptional strength, electrical conductivity, and thermal properties, PETG is further enhanced, yielding the composite material known as Graphene-Reinforced PETG (G-PETG)^{4–6}. Numerous studies have investigated various composites combined with PETG for different applications. Patel et al.⁷ explored the influence of FDM process parameters layer thickness, raster angle, and printing speed on the mechanical properties of carbon fiber (CF) reinforced PETG. Optimal settings, such as a 0° raster angle, 0.2 mm layer thickness, and 40 mm/s speed, enhanced tensile and flexural strength due to improved material bonding. Lower raster angles, reduced layer thickness, and slower speeds further improved mechanical properties. The study also found a 30% increase in tensile strength when CF was incorporated into recycled Polyethylene Terephthalate (PET) waste, highlighting potential applications in automotive and defense sectors for improved performance and sustainability. Jacob et al.⁸ conducted a technical-economic study on optimizing FDM parameters for the

¹Centre for Sustainable Materials and Surface Metamorphosis, Chennai Institute of Technology, Chennai 600069, Tamilnadu, India. ²Department of Mathematics, School of Advanced Science, Vellore Institute of Technology, Vellore, India. ³Masters of Engineering in Engineering Management, Lockheed Martin Engineering Management, University of Colorado, Boulder, CO 80308, USA. ⁴School of Mechanical Engineering, Vellore Institute of Technology, Chennai 600127, Tamilnadu, India. ⁵College of Engineering and Agro-Industrial Technology, Arba Minch University, Sawla Campus, Arba Minch, Ethiopia. ✉email: sraja@citchennai.net; simon.yishak@amu.edu.et

production of PETG and Acrylonitrile Styrene Acrylate (ASA) parts, focusing on layer height (L_h) and infill percentage (I_d). Using value analysis, which maximizes the ratio between mechanical performance (V_i) and production cost (C_p), they found that for PETG tensile specimens, the most influential factor was layer height, while for compression specimens, infill percentage had a greater impact. In ASA parts, the infill percentage was the key factor for both tensile and compression specimens. The study identified optimal FDM parameters 0.20 mm layer height and 100% infill. Bedi et al.⁹ examined the effects of varying graphene compositions (0.02, 0.04, 0.06, 0.08, and 0.1 wt%) on the sliding wear properties of 3D-printed PETG composites using FDM and ASTM G99-05 guidelines. The composites were prepared via a twin-screw extruder, producing filaments with a 1.75 mm diameter. The study employed a pin-on-disc tribometer to assess sliding wear characteristics under a 10 N load, 70 mm wear track, and 300 r/min speed. Results revealed that increasing graphene content (0.06 to 0.1 wt%) significantly reduced the coefficient of friction but had limited impact on minimizing specific wear rate (SWR). The 0.04 wt% graphene composite showed the lowest SWR among the compositions but still higher than pure PETG. Further investigation is needed to clarify these discrepancies. Bedi et al. focused on improving the sliding wear properties and friction of graphene-reinforced PETG, while our study optimizes the mechanical properties of G-PETG components using AHP for additive manufacturing. Raja et al.¹⁰ highlighted the transformative impact of additive manufacturing on production efficiency and material waste reduction, focusing on optimizing the mechanical properties of G-PETG impellers. By employing FAHP and TOPSIS to identify optimal printing parameters, the study achieved a 15% increase in tensile strength and a 12% decrease in production time, resulting in superior surface finish and structural integrity for high-performance applications. Raja et al. utilized the FAHP-TOPSIS method to optimize the mechanical properties and production efficiency of G-PETG impellers, whereas our study employs the Spice Logic AHP for a comparative analysis of FDM parameters with separate samples preparation in enhancing G-PETG components.

The optimization of G-PETG composites through advanced additive manufacturing techniques has demonstrated significant potential for enhancing material performance. This combination offers improved mechanical properties, making G-PETG a promising candidate for high-performance applications in industries such as aerospace, automotive, and energy storage¹¹⁻¹³. Different optimization techniques can be employed to either enhance or reduce specific outcomes. For instance, in scenarios where time is critical, the objective often shifts to minimizing results. Conversely, when the emphasis is on improving tensile mechanical properties, the focus is on maximizing these outcomes. However, the complexity and cost of statistical optimization models, which include expenses for raw materials and testing, can be significant. Therefore, this research suggests leveraging the Multi-Criteria Decision-Making (MCDM) method along with a rating system. Despite the advantageous properties of G-PETG, optimizing the mechanical performance of components fabricated using this material remains a challenge due to the numerous variables involved in the FDM process, such as printing temperature, layer height, infill density, and print speed. To address this, advanced decision-making tools, such as the Analytical Hierarchy Process (AHP) by spice logic, can be employed to systematically identify the optimal combination of parameters that yield superior mechanical performance^{14,15}. Impellers serve as crucial components across numerous industries, such as water pumping, chemical processing, and mining, where they are vital for enhancing the flow and pressure of fluids. In pumping systems, these components not only aid in energy extraction but also play a significant role in regulating flow dynamics and pressure levels^{16,17}. Traditionally, impellers were manufactured from metals and alloys; however, there has been a noticeable shift toward thermoplastic polymers and composite materials over the last few decades¹⁸. This transition is primarily attributed to the benefits of reduced weight, cost efficiency, and simplified manufacturing processes that these materials provide.

A comparative study conducted by Chew et al.¹⁹ assessed impellers made from both metallic and non-metallic materials, focusing on thermoplastics such as polyether ether ketone (PEEK), polyether ketone (PEK), and carbon fiber-reinforced PEEK (CFR-PEEK). Their research revealed that CFR-PEEK offers superior resistance to corrosion and erosion, lowers volumetric leakage, and minimizes both weight and rotor shaft deflection. In another investigation, Hernandez Carrillo et al.²⁰ examined impellers made from acrylonitrile butadiene styrene (ABS), finding that these impellers can endure strains of up to 4 bar and tensions of 2.5 bar. Additionally, Polak et al.²¹ fabricated a water pump impeller using ABS that operated effectively at speeds of 2950 rpm.

This current research aims to enhance the fabrication process of impellers using G-PETG, a material that has not been extensively researched for this application. G-PETG, recognized for its amorphous structure, is being investigated as a viable alternative to other reinforced polymers due to its improved printability, lower risk of nozzle clogs, and increased toughness compared to conventional PETG. For this purpose, a composite comprising 5% graphene and 95% PETG was developed, pelletized, and utilized as filament in the FDM process for producing rotating component.

A key innovation of this study is the application of MCDM techniques, specifically the Spice Logic AHP method, to optimize the 3D printing parameters of G-PETG filament within Material Extrusion (MEx) processes. By prioritizing mechanical property enhancement, the research addresses crucial challenges in additive manufacturing, such as improving material performance and process efficiency. The main objective is to establish a framework that not only enhances the mechanical properties of G-PETG printed parts but also optimizes the associated process parameters to lower production costs and time. This innovative approach effectively links theoretical models to practical applications in additive manufacturing, providing a scalable solution for high-performance needs in various industries. Comprehensive details regarding the materials and methods, printing and testing procedures, and results discussions are provided to fulfill the study's goals.

Materials and methods

Assumption and alternative preparation

- The process parameters in additive manufacturing, particularly in the context of FDM, significantly influence the mechanical properties and overall quality of the final product²². These parameters, including printing temperature, printing speed, layer height, and infill density, interact in complex ways, forming clusters of influences that can enhance or degrade the performance of the printed component. For instance, maintaining an optimal printing temperature is crucial to ensure proper filament melting and deposition. If the temperature is set too low, the filament may not melt sufficiently, leading to poor layer adhesion, under-extrusion, and potential clogging of the nozzle. Conversely, if the printing speed is too high, it may not allow adequate time for each layer to bond properly, resulting in weak interlayer adhesion and increased likelihood of defects such as warping or delamination. Thus, a careful balance of these parameters is essential to produce high-quality parts with desirable mechanical properties. By considering these parameters as a cluster, the study acknowledges their interdependent nature and the necessity of optimizing them collectively to achieve the best possible outcomes in G-PETG impeller production.
- To identify the appropriate cluster of process parameters, the mechanical properties required for the impeller, such as ultimate tensile strength (C1), Young's modulus (C2), ultimate flexural strength (C3), and ultimate compression strength (C4), have been chosen as criteria due to the specific application requirements. The selection of appropriate process parameters is crucial in additive manufacturing to ensure that the final product meets the required performance standards. For the production of G-PETG impellers, the mechanical properties such as ultimate tensile strength (C1), Young's modulus (C2), ultimate flexural strength (C3), and ultimate compression strength (C4) are critical criteria²³. These properties have been chosen based on the specific application requirements of impellers, which are typically subjected to various mechanical stresses during operation. Ultimate tensile strength (C1) is essential for determining the maximum stress that the impeller material can withstand while being stretched or pulled before breaking. This property ensures that the impeller can handle high rotational speeds and resist deformation under tensile loads. Young's modulus (C2) measures the stiffness of the material, indicating its ability to deform elastically under stress. A higher Young's modulus implies that the impeller will maintain its shape and structural integrity under operational forces, which is vital for maintaining performance and efficiency in fluid dynamics. Ultimate flexural strength (C3) represents the material's ability to resist deformation under bending or flexural loads. This property is particularly important for impellers, which may experience bending stresses due to fluid forces and rotational movement. Ensuring high flexural strength helps in preventing cracks and failures during service. Ultimate compression strength (C4) indicates the material's capacity to withstand compressive loads without collapsing. This property is crucial for impellers that may be subjected to compressive forces during assembly, operation, or maintenance. High compressive strength ensures that the impeller can endure these stresses without compromising its structural integrity. By focusing on these key mechanical properties, the study aims to optimize the additive manufacturing process parameters to produce impellers that meet the rigorous demands of their application. Employing an AHP methodology by Spice Logic provides a systematic and robust approach to evaluating and prioritizing these criteria, ensuring that the selected process parameters lead to the highest performance and reliability of the final product.
- The range of printing parameter values adopted in this study is derived from a comprehensive analysis of previous research on additive manufacturing with G-PETG material. Prior studies have consistently highlighted the significance of optimizing key parameters such as print speed, travel speed, layer height, infill density, extruder temperature, and platform temperature to achieve superior mechanical properties and dimensional accuracy in printed components. These parameters were meticulously selected based on their proven influence on the quality and performance of the final product. For instance, studies²⁴ have demonstrated that variations in print speed and travel speed can significantly impact the surface finish and structural integrity of printed parts. Similarly, research by²⁵ has established that layer height and infill density play crucial roles in determining the strength and weight of the manufactured components. Furthermore, the extruder and platform temperatures are critical in ensuring proper layer adhesion and minimizing warping, as evidenced by the findings of^{10,24,25}. Table 1 outlines the specific parameter values used for printing the testing specimens in this study, ensuring a comprehensive exploration of the parameter space. These values are strategically selected to encompass a broad range of settings, enabling a robust analysis of their effects on the production performance of G-PETG impellers. By leveraging the insights gained from previous studies, this research aims to identify the optimal combination of parameters that enhances the mechanical properties and efficiency of the additive manufacturing process for G-PETG material.
- In the context of optimizing manufacturing parameters for the production of G-PETG impellers, it is crucial to identify and prioritize criteria that contribute positively to the overall performance and efficiency of the process. The assumption that all selected criteria are considered beneficial is based on the premise that each criterion, when optimized, will enhance the desired outcomes of the manufacturing process. Beneficial criteria are those that directly or indirectly improve the quality, efficiency, and effectiveness of the production. For instance, criteria such as nozzle temperature, print speed, and infill density play significant roles in determining the mechanical properties, surface finish, and structural integrity of the final product. By optimizing these parameters, the production process can achieve higher precision, reduced material wastage, and improved durability of the impellers. Additionally, criteria like energy consumption and cost-effectiveness are essential for ensuring that the manufacturing process is sustainable and economically viable. The use of the AHP methodology further supports this assumption by providing a structured approach to evaluate and prioritize these beneficial criteria. AHP allows for a comprehensive analysis of each criterion's relative importance, ensuring that the optimization process is aligned with the overarching goals of enhancing production

performance. By focusing on beneficial criteria, the research aims to achieve a balanced optimization that not only meets technical requirements but also aligns with environmental and economic considerations. Overall, the assumption that all selected criteria are beneficial is integral to the holistic approach adopted in this study, where each criterion is carefully chosen for its positive impact on the manufacturing process and the quality of the G-PETG impellers.

- The Pratham 6.0 printer and Flashforge slicing software were utilized to print the testing specimens. It is important to recognize that research outcomes may vary if other technologies are employed due to several factors. Firstly, different 3D printers have unique mechanical and operational characteristics that can influence the accuracy, precision, and overall quality of the printed components. Variations in extruder design, build volume, and motion systems can lead to differences in the final printed product. Additionally, slicing software plays a crucial role in the additive manufacturing process by converting digital models into instructions for the printer. Different slicing algorithms and settings can affect layer height, infill patterns, and support structures, which in turn impact the mechanical properties and dimensional accuracy of the printed specimens. As a result, the specific combination of the Pratham 6.0 printer and Flashforge slicing software used in this study provides a controlled environment for optimizing the manufacturing parameters for G-PETG impeller production. However, it is acknowledged that employing different 3D printing technologies and slicing software may yield variations in research outcomes, and thus the findings of this study should be interpreted within the context of the specific equipment and software used.
- The selection of the “Line” printing pattern in this study is driven by its efficiency in terms of raw material consumption compared to other complex patterns. The “Line” pattern, characterized by its straightforward and linear deposition of material, minimizes waste and optimizes the use of filament. This is particularly advantageous in additive manufacturing where material costs and resource efficiency are critical considerations. In contrast, more intricate patterns such as gyroid, triangle, and hexagonal, although beneficial for certain structural properties, inherently require a greater volume of raw materials. These complex patterns involve more extensive infill structures, leading to increased material usage and potentially higher production costs. Additionally, the increased complexity of these patterns can impact the print time and the mechanical properties of the final product, introducing variables that may alter the research outcomes. By adopting the “Line” printing pattern, this study ensures a controlled and consistent use of materials, allowing for a more precise assessment of the impact of additive manufacturing parameters on the production performance of G-PETG impellers. This approach not only aligns with the objectives of optimizing production efficiency but also supports sustainable manufacturing practices by reducing material wastage.
- In this study, the term “Alternative” denotes a cluster of parameters, which is essential for the optimization process in additive manufacturing. Each alternative is defined by a unique combination of process parameters that collectively influence the quality and performance of the produced G-PETG impellers. This approach allows for a systematic investigation of how different parameter clusters affect the manufacturing outcomes. By considering clusters of parameters as alternatives, we can effectively analyze the interplay between variables such as nozzle temperature, print speed, layer height, and infill density. This methodology provides a comprehensive understanding of the parameter space, facilitating the identification of optimal settings for enhancing production performance. Moreover, grouping parameters into clusters simplifies the experimental design, enabling more efficient data collection and analysis. This assumption aligns with the principles of the AHP employed in this study, as it allows for the structured evaluation and prioritization of multiple criteria simultaneously. Ultimately, treating parameter clusters as alternatives ensures a robust and scalable approach to parameter optimization in additive manufacturing.

The composite material used in this study, G-PETG was developed by incorporating graphene into a PETG polymer matrix. To achieve uniform dispersion of graphene throughout the PETG, a single-screw extrusion process was employed. This process ensured that the graphene particles were consistently distributed within the PETG matrix, creating a homogenous composite material that would enhance the mechanical properties of the printed components. The preparation process began with the mixing of graphene powder and PETG granules in a pre-determined ratio, followed by feeding this mixture into a single-screw extruder. The extruder operated at carefully controlled temperatures and screw speeds to melt and blend the materials effectively. As the material passed through the extruder, the graphene became thoroughly dispersed in the molten PETG, ensuring consistent reinforcement. The extruded composite was then passed through a cooling system to solidify the material before being pelletized into small, manageable granules. These granules were subsequently re-extruded to form a filament with a diameter of 1.75 mm, which is standard for most FDM 3D printers. The filament was cooled and spooled, ready for use in 3D printing processes. The entire extrusion alternative preparation process, including the filament production, is depicted in Fig. 1, which outlines the steps of composite preparation from raw material to finished filament.

The G-PETG filament was then used to fabricate test specimens using a Pratham 6.0 FDM 3D printer via nozzle diameter of 0.4 mm. Flashforge slicing software was employed to design the specimens and control the printing parameters, including layer height, printing speed, nozzle temperature, and bed temperature. The selection of the cluster of process parameters, as detailed in the Table 1, was based on a comprehensive evaluation of how these parameters influence the mechanical properties and overall quality of the fabricated specimens. The specific combination of print speed, travel speed, layer height, infill density, extruder temperature, platform temperature, and infill pattern was optimized to balance efficient printing time with the mechanical performance of the final parts. Each parameter plays a crucial role in determining the structural integrity, surface finish, and overall performance of the 3D-printed components.

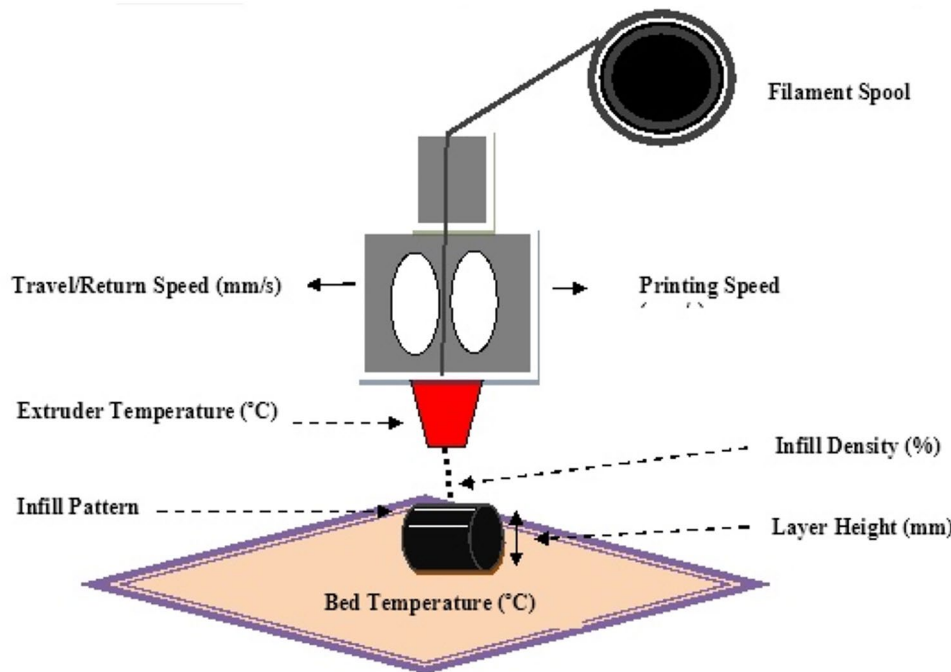


Fig. 1. Process flow for sample preparation.

Process parameter	Units	Alternative 1	Alternative 2	Alternative 3	Alternative 4	Alternative 5
Print speed	mm/s	30	40	50	60	70
Travel speed	mm/s	80	85	90	95	100
Layer height	mm	0.3	0.25	0.2	0.15	0.1
Infill density	%	55	60	65	70	75
Extruder temperature	°C	230	235	240	245	250
Platform temperature	°C	80	85	90	95	100
Infill pattern	Line					

Table 1. Process parameter taken for G-PETG^{3,10}.

Individual process parameter overview

- Print Speed (mm/s): Print speed refers to how fast the printer head moves while extruding material. In this study, print speeds ranged from 30 mm/s to 70 mm/s, allowing for flexibility between producing fine details and faster build times. Higher speeds can reduce print time but may compromise surface quality, while lower speeds enhance layer adhesion and precision²⁶.
- Travel Speed (mm/s): Travel speed refers to the speed at which the printer head moves when it is not extruding material. This was varied from 80 mm/s to 100 mm/s to minimize non-printing movement time while preventing issues such as stringing or poor adhesion due to overly rapid movement²⁶.
- Layer Height (mm): Layer height directly affects print resolution and surface finish. The tested values of 0.10 mm to 0.30 mm represent a trade-off between higher resolution prints and faster build times. Lower layer heights, such as 0.10 mm, improve surface quality but increase the print time, while higher layer heights can lead to a rougher finish but faster production²⁷.
- Infill Density (%): Infill density determines the internal structure of the printed object, contributing to its strength and weight. In this study, densities ranged from 55 to 75%, where higher infill percentages result in sturdier and more rigid parts, while lower percentages reduce material usage and print time but may compromise mechanical strength²⁷.
- Extruder Temperature (°C): The extruder temperature was varied between 230°C and 250°C to optimize the flow of the G-PETG material. Higher temperatures improve layer bonding and reduce the risk of clogging, but excessive temperatures can cause filament degradation, affecting the part's mechanical properties²⁸.
- Platform Temperature (°C): The platform temperature, ranging from 80°C to 100°C, ensures proper adhesion of the first layer and minimizes warping during the printing process. A higher platform temperature improves adhesion, particularly for larger prints or materials like PETG that tend to warp during cooling²⁸.

- Infill Pattern (Line): The infill pattern used was line, which provides a good balance between mechanical strength and material efficiency. The line pattern supports uniform stress distribution throughout the part and can be printed faster than more complex infill patterns such as honeycomb or grid²⁸.

The selection of this specific cluster of process parameters is based on their combined ability to improve both the mechanical performance and efficiency of the production process. The use of a 0.20 mm layer height and 65% infill density provided an optimal balance between mechanical strength and reasonable print time, making it suitable for applications that require durable parts with minimal production time. The 240 °C extruder temperature ensured proper flow and adhesion of the G-PETG material without risking thermal degradation, while the 90 °C platform temperature minimized warping and ensured strong adhesion of the first layer.

By fine-tuning each parameter, the printing process was optimized to achieve superior mechanical properties, such as improved tensile and flexural strength, while maintaining efficient production. This cluster was designed to harness the full potential of the graphene-reinforced PETG composite for high-performance applications, ensuring reliable and repeatable results.

These parameters were optimized to ensure the best possible mechanical properties for the printed parts, especially considering the unique properties of the graphene-reinforced composite. Figure 2 highlights the key 3D printing parameters in the extrusion process, such as nozzle temperature, printing speed, and layer height. These parameters play a vital role in controlling material flow, layer bonding, and overall print quality. Optimizing these settings ensures better structural integrity, surface finish, and material efficiency in the final product.

Mechanical testing standards and equipment

To comprehensively evaluate the mechanical properties of the G-PETG composite, various tests were conducted, including tensile, flexural, and compression tests. Each test followed industry-standard protocols to ensure that the results were accurate and comparable to other studies. The tensile properties of the G-PETG composite were evaluated using the ASTM D638 type V standard, which is specifically designed for polymeric materials. Type V specimens were chosen due to their smaller gauge length, making them ideal for testing the relatively thin sections produced by 3D printing. The specimens were printed in accordance with the dimensions specified in the standard, ensuring consistent and reliable data. The tests were carried out on a Tinius Olsen H10KL universal testing machine, with a loading rate of 1 mm/min, as per the standard requirements. Tensile properties such as ultimate tensile strength (UTS), elongation at break, and Young's modulus were recorded. Flexural properties were measured using the ISO 178/ASTM D790 standard, which is widely accepted for determining the flexural strength and modulus of polymer-based materials. This test involved applying a three-point bending load to the specimens until failure, providing insight into the material's ability to withstand bending forces. The G-PETG specimens were printed with dimensions conforming to the ASTM D790 standard, and the tests were conducted at a loading rate of 1 mm/min. Compression testing was performed according to the ASTM D695 standard, which is used to evaluate the compressive strength of reinforced and unreinforced plastics. This test assessed the material's ability to resist compressive loads, which is crucial for components like impellers that experience significant compressive stresses during operation. Compression test specimens were printed in compliance with ASTM D695 dimensions, and the Instron machine was used with a 1 mm/min loading rate to ensure consistency across all mechanical tests. The printed specimens were conditioned at room temperature for 48 h prior to testing

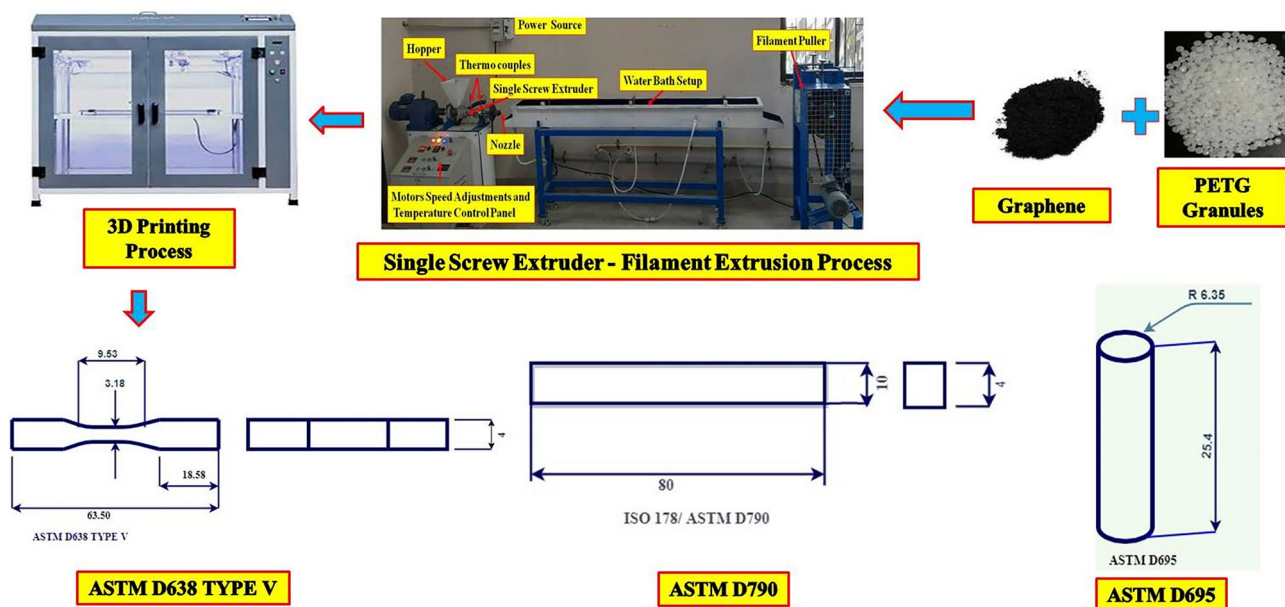


Fig. 2. Printing parameters of 3D printing extrusion process.

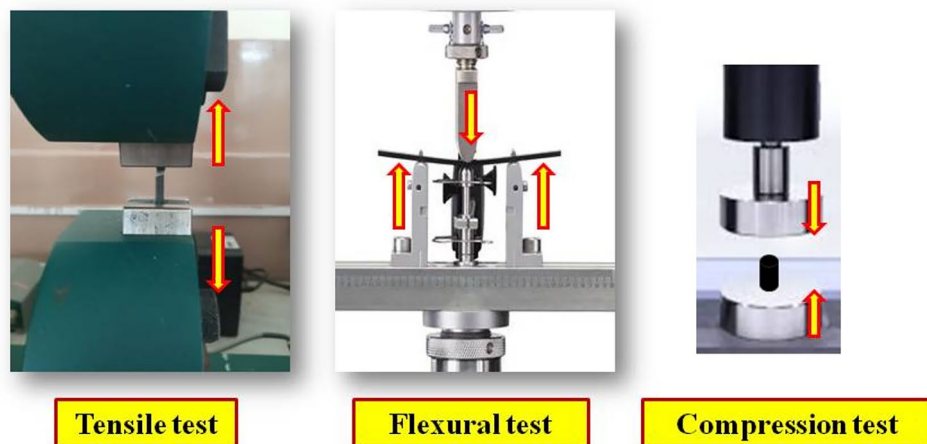


Fig. 3. Experimental setup.

TRIAL	I	II	III	Average	Importance
UTS (MPa), (A-Alternatieve)	A- 1	52.3	51.7	50.4	VL
	A- 2	63.4	62.2	60.1	H
	A- 3	57.2	62.4	69.1	VH
	A- 4	60.7	64.1	56.8	A
	A- 5	52.4	59.2	64.7	L

Table 2. Tensile test UTS observation.

to eliminate any residual stresses from the printing process. Each test was conducted in triplicate to ensure the accuracy and repeatability of the results. The tensile, flexural, and compression tests provided a comprehensive view of the mechanical performance of the G-PETG composite, allowing for a thorough comparison with other polymeric and composite materials. Figure 3 presents the experimental setup for tensile, flexural, and compression tests. These setups are designed to assess the mechanical properties of the printed materials, such as strength, stiffness, and deformation under various loads.

After testing, the data collected from each mechanical test was analyzed to determine key mechanical properties such as ultimate tensile strength, Young's modulus, flexural strength, and compressive strength. Statistical analysis was performed to ensure the reliability of the results, and the optimal printing parameters were identified based on these findings. The mechanical properties of the G-PETG composite were then compared to those of conventional PETG and other thermoplastic composites, providing insight into the effectiveness of graphene reinforcement in improving material performance. By utilizing a rigorous testing methodology and adhering to established standards, this study aimed to provide a reliable assessment of the mechanical properties of G-PETG for potential applications in industries that demand high-performance materials, such as aerospace, automotive, and energy storage.

In this study, the categorization of alternatives based on their ultimate tensile strength (UTS) is essential for assessing the material's mechanical performance. Alternatives exhibiting low UTS values are classified under the category of "Very Low" (VL), indicating a weaker structural performance and lower resistance to tensile forces. This classification is crucial for distinguishing materials that may not be suitable for applications requiring high mechanical strength and Table 2 shows the observation of UTS.

On the other hand, alternatives with superior UTS values are categorized as "Very High" (VH), denoting their exceptional tensile strength and potential suitability for high-stress applications. This clear classification allows for a systematic comparison of different materials or process parameters, aiding in the selection of optimal conditions for additive manufacturing.

Additionally, the study evaluates the stiffness of the materials through Young's modulus. The results for Young's modulus, which measure the material's resistance to deformation under stress, are presented comprehensively in Table 3, providing insight into how different alternatives perform in terms of elasticity and rigidity.

Multi criteria decision making (MCDM)

Multi-Criteria Decision Making (MCDM) encompasses a suite of advanced mathematical techniques designed to assist in selecting the optimal solution from a set of alternatives, based on multiple criteria, each with varying levels of importance. This methodology has garnered significant attention across diverse fields such as healthcare, defense, operations management, information technology, disaster response, and energy systems, where it is often applied for decision-making tasks involving selection, evaluation, and prioritization of alternatives²⁹.

TRIAL		I	II	III	Average	Importance
Young's Modulus (MPa)	A- 1	635	661	618	638	L
	A- 2	644	674	614	644	A
	A- 3	692	729	786	735.6	VH
	A- 4	725	748	719	730.6	H
	A- 5	624	608	627	619.6	VL

Table 3. Young's Modulus observation.

In this research, MCDM is applied to optimize the process parameters for Fused Deposition Modeling (FDM) in additive manufacturing. The study begins with a thorough review of how MCDM techniques have been employed in previous research within the context of additive manufacturing processes³⁰. Among various MCDM approaches such as the Technique for Order of Preference by Similarity to Ideal Solution (TOPSIS), VIKOR, and DEMATEL^{21,27–29} the Analytical Hierarchy Process (AHP) has been selected as the primary decision-making tool for this study.

The specific software employed in this research is Spice Logic's AHP, known for its intuitive interface and powerful capabilities, including handling inconsistencies, identifying errors, and calculating standard deviations. Several prior studies have utilized Spice Logic AHP for a variety of decision-making and optimization applications³¹. The rationale behind choosing this tool lies in its comprehensive features, which are well-suited for complex decision-making processes. This study represents a novel application of Spice Logic AHP in optimizing the Material Extrusion (MEx) process parameters for the production of impellers using Graphene-Reinforced PETG (G-PETG). No prior research has investigated the use of Spice Logic AHP in this specific context, making this study a pioneering effort in the field. The upcoming sections will provide an in-depth explanation of the research methodology, including detailed procedures for 3D printing and mechanical testing.

Result and discussion

To select the appropriate process parameters, statistical methods are often employed, with the Taguchi method being a popular choice due to its effectiveness in optimizing complex systems. This method usually involves conducting at least nine distinct experiments, organized in an L9 orthogonal array, to systematically evaluate various parameter combinations. The goal is to manage variability and uncertainty, enabling the identification of optimal process settings. In this study, a total of 27 alternatives were produced, with 3 alternatives prepared for each of the 9 experimental setups, focusing specifically on assessing tensile strength. Among these, the third alternative emerged as the best performer, achieving an ultimate tensile strength of 62.9 MPa. This remarkable result was influenced by the specific combination of five process parameters, which had a significant impact on the material's mechanical properties. Additionally, this same alternative exhibited the highest Young's modulus, highlighting its superior stiffness compared to the others, demonstrating the importance of process optimization in achieving enhanced material performance.

Alternative 2 demonstrated superior flexural strength, achieving a notable measurement of 82.3 MPa. This impressive performance highlights the material's ability to withstand bending forces without yielding, making it particularly valuable in applications where resistance to flexural stress is crucial. Conversely, alternative 5 showcased the highest ultimate compressive strength, reaching an impressive 86.6 MPa. This strength indicates the alternative's remarkable capacity to endure axial loads without failure, showcasing its potential for use in structural applications where compressive forces are prevalent. These results underscore the significant variations in mechanical properties among different alternatives, emphasizing the importance of optimizing process parameters to enhance both flexural and compressive strengths in material formulations. The distinct performance characteristics of these alternatives indicate their suitability for diverse engineering applications, where specific mechanical properties are critical for operational effectiveness.

When evaluating the ultimate tensile strength using the rating method, the results indicate that alternative 1 has the lowest tensile strength among the tested specimens. This is followed in ascending order by alternatives 5, 4, and 2. In terms of Young's modulus, alternative 5 again ranks lowest, with alternative 1 coming next, followed by alternatives 2 and 4, indicating a variation in stiffness across the alternatives.

For ultimate flexural strength assessments, alternative 5 is identified as having the weakest performance, succeeded by alternatives 4, 1, and 3 in that order. This trend highlights the differing mechanical properties observed in the alternatives. Finally, when analyzing ultimate compression strength, alternative 1 shows the least strength, with alternatives 4, 2, and 3 following sequentially. These findings illustrate significant disparities in the mechanical properties across the alternatives, underlining the importance of selecting optimal parameters for enhanced performance in various loading conditions. Table 4 presents the observations from the flexural test, which evaluates the bending strength and stiffness of the printed specimens.

Following the initial analysis, a Pairwise Comparison Matrix was developed to evaluate the various criteria against the alternatives, utilizing the fuzzy terms approach as outlined by the Spice Logic Analytical Hierarchy Process (AHP). This matrix serves as a systematic tool for comparing the selected criteria in pairs, allowing for a comprehensive assessment of their relative importance. Table 5 presents the observations from the compression test, detailing key measurements such as compressive strength, modulus, and deformation at failure.

TRIAL		I	II	III	Average	Importance
UFS (MPa)	A- 1	74	82	86	80.6	A
	A- 2	82	76	89	82.3	VH
	A- 3	82	76	87	81.6	H
	A- 4	72	78	84	78	L
	A- 5	79	82	72	77.6	VL

Table 4. Flexural test observation.

TRIAL		A	B	C	Average	Importance
UCS (MPa)	A- 1	68	76	72	72	VL
	A- 2	78	72	75	75	A
	A- 3	82	86	88	85.3	H
	A- 4	69	74	79	74	L
	A- 5	80	84	96	86.6	VH

Table 5. Compression test observation.

Criteria Vs Criteria Evaluation	Ultimate Tensile Strength	Young's Modulus	Ultimate Flexural Strength	Ultimate Compression Strength
Ultimate Tensile Strength	1	0.333	0.2	0.25
Young's Modulus	3	1	0.6	0.75
Ultimate Flexural Strength	5	1.66	1	1.25
Ultimate Compression Strength	4	1.33	0.8	1
Criteria Weight	0.560	0.186	0.112	0.14

Table 6. Pairwise matrix for Criteria evaluation

Table 6 Presents the constructed pairwise matrix, which reflects the evaluation of the chosen criteria. In this matrix, the criteria are systematically compared to one another based on the Saaty scale, a widely recognized method for prioritizing decision-making factors. The Saaty scale employs a numerical rating system that ranges from 1 to 9, enabling the decision-maker to express their preferences in a quantifiable manner. A score of 1 indicates equal importance between two criteria, while higher values signify an increasing level of preference for one criterion over the other. By employing this structured comparison method, the study ensures that the evaluation of each criterion is thorough and grounded in a systematic analytical framework, ultimately facilitating the selection of the most suitable alternatives.

In this study, the selection of importance ratings follows the Saaty scale, which assigns values from 1 to 5 to evaluate the significance of various criteria. In Table 6, specifically in the second column and second column, a moderate level of importance was determined based on the average observations collected during the assessment. It is essential to clarify that the scale utilized ranges from 1, indicating very low importance, to 5, denoting very high importance, adhering to the transitivity rule.

Once the importance ratings were systematically assigned to each criterion, the process for calculating criterion weights involved a straightforward mathematical operation. The maximum value within each criterion group was divided by the individual criterion values, resulting in column-wise sums that represent the weights of each criterion. Notably, the weight assigned to the criterion “Ultimate Tensile Strength” was calculated to be 0.560, underscoring its substantial impact on the overall evaluation process. This systematic approach ensures that the most critical factors are appropriately weighted, enhancing the robustness of the decision-making framework employed in this research.

Table 7 Presents the pairwise comparison matrix used for evaluating alternatives based on the first criterion, which is the UTS. In this matrix, the selected alternatives are systematically compared against each other, utilizing the Saaty scale for assessing their relative importance. For instance, at the intersection of column three and column two, a ranking of intermediate importance is assigned, indicating a position that lies between moderate and strong significance according to the Saaty scale. This conclusion was drawn from the notable ratings recorded during the evaluation process.

Once the importance ratings for each alternative are established based on the UTS criterion, the maximum value within each column is divided by the individual values of that column. This calculation ensures that the sum of the priority values across the column equals 1. For instance, the priority value for “Alternative 1” is calculated to be 0.06, reflecting its substantial role in the overall evaluation process by using Eq. 1. This systematic approach highlights the significance of each alternative in relation to the defined criterion, facilitating a clear understanding of their relative merits.

Ultimate Tensile Strength 0.56	Alternative 1	Alternative 2	Alternative 3	Alternative 4	Alternative 5
Alternative 1	1	4	5	3	2
Alternative 2	0.25	1	1.25	0.75	0.5
Alternative 3	0.2	0.8	1	0.6	0.4
Alternative 4	0.333	1.333	1.666	1	0.666
Alternative 5	0.5	2	2.5	1.5	1
Priorities	0.06	0.266	0.333	0.2	0.133

Table 7. Pairwise matrix for alternatives evaluation based on Criteria 1.

Young's Modulus (Ym) 0.186	Alternative 1	Alternative 2	Alternative 3	Alternative 4	Alternative 5
Alternative 1	1	3	5	4	0.5
Alternative 2	0.333	1	1.666	1.333	0.166
Alternative 3	0.2	0.6	1	0.8	0.1
Alternative 4	0.25	0.75	1.25	1	0.125
Alternative 5	2	6	10	8	1
Priorities	0.074	0.222	0.37	0.296	0.037

Table 8. Pairwise matrix for alternatives evaluation based on Criteria 2.

Ultimate Flexural Strength 0.112	Alternative 1	Alternative 2	Alternative 3	Alternative 4	Alternative 5
Alternative 1	1	5	4	2	0.33
Alternative 2	0.2	1	0.8	0.4	0.06
Alternative 3	0.25	1.25	1	0.5	0.083
Alternative 4	0.5	2.5	2	1	0.166
Alternative 5	3	15	12	6	1
Priorities	0.081	0.405	0.324	0.162	0.027

Table 9. Pairwise matrix for alternatives evaluation based on Criteria 3.

$$\lambda_{\max} = \frac{\text{the total of the ratios between the weighted sum values and the criteria weights}}{\text{number of criteria}} \quad (1)$$

Table 8 Outlines the pairwise comparison matrix utilized for assessing the alternatives based on the second criterion, which is Young's Modulus. In this evaluation, selected alternatives are systematically compared against one another using the Saaty scale, which facilitates a structured assessment of relative importance according to the Young's Modulus outcomes. For example, examining the entry at the intersection of the third column and the second column in table 8 reveals a moderate level of significance as per the Saaty scale. This assessment is based on the average ratings collected throughout the evaluation.

Once the importance scales for all alternatives have been meticulously assigned in relation to criterion 2, the next step involves calculating the Priorities value for each alternative. This is achieved by dividing the maximum value within each alternative column by the individual values of that column. This calculation ensures that the cumulative sum of the values in each column equates to the Priorities value 2. For instance, the Priorities value for "Alternative 1" is calculated to be 0.074, highlighting its substantial role in the overall evaluation framework and emphasizing its relevance in the decision-making process. This structured approach not only clarifies the comparative importance of each alternative but also lays the groundwork for informed decisions based on mechanical property evaluations.

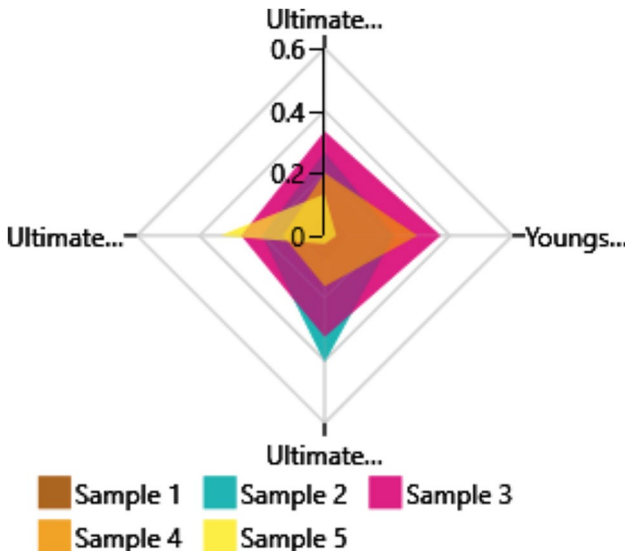
Table 9 Presents the pairwise comparison Matrix used for evaluating alternatives based on Criterion 3, which is centered on Ultimate Flexural Strength. In this matrix, the selected alternatives are assessed through the lens of the Saaty scale, which relies on the results obtained for Ultimate Flexural Strength. For instance, the entry found at the intersection of the third column and the second column in table 9 denotes a strong significance according to the Saaty scale. This evaluation arises from identifying a "Very High" rating during the assessment phase, indicating a clear distinction in performance between the alternatives.

After systematically assigning importance ratings to each alternative in relation to Criterion 3, the highest value from each alternative is divided by its respective individual values. This division process guarantees that the total of these values calculated column -wise results in a Priorities value of 3. Specifically for "Alternative 1," the calculated Priorities value is 0.081. This Table 9 underscores Alternative 1's considerable impact in the

Ultimate Compression Strength 0.14	Alternative 1	Alternative 2	Alternative 3	Alternative 4	Alternative 5
Alternative 1	1	3	4	2	5
Alternative 2	0.333	1	1.333	0.666	1.666
Alternative 3	0.25	0.75	1	0.5	1.25
Alternative 4	0.5	1.5	2	1	2.5
Alternative 5	0.2	0.6	0.8	0.4	1
Priorities	0.066	0.2	0.266	0.133	0.333

Table 10. Pairwise matrix for alternatives evaluation based on Criteria 4.

Alternatives	Alternative 1	Alternative 2	Alternative 3	Alternative 4	Alternative 5
Priorities	0.07	0.265	0.33	0.204	0.131
Ranking	V	II	I	III	IV

Table 11. Ranking matrix.**Fig. 4.** Change the criteria weight of C1/C4.

overall evaluation, highlighting its relevance in the context of Ultimate Flexural Strength comparisons among the alternatives.

Table 10 Provides a detailed pairwise comparison Matrix for assessing alternatives in relation to Criterion 4, which centers on Ultimate Compression Strength. The evaluation begins with a comparative analysis of the selected alternatives, utilizing the Saaty scale based on the results for Ultimate Compression Strength. For example, in table 10, the value at the intersection of column three and column two suggests a moderate level of importance, as determined by an average rating during the evaluation phase.

Following this initial comparison, the importance scales are meticulously assigned to all alternatives in accordance with Criterion 4. To derive the Priorities value, the maximum value for each alternative is divided by its corresponding individual values. This method ensures that the sum of these values across each column results in the Priorities value for Criterion 4. In the case of “Alternative 1,” the calculated Priorities value is 0.066, highlighting its notable impact within the overall evaluation framework. This structured approach not only clarifies the significance of each alternative but also facilitates a more informed decision-making process regarding material selection based on Ultimate Compression Strength.

Table 11 Presents a comprehensive ranking of the alternatives, which was derived through a systematic process that involves summing the priority values and multiplying them by the respective weights assigned to each criterion. This ranking methodology allows for a clear comparison between the alternatives, where those that receive higher priority values are given the top ranks, indicating their greater overall significance in the context of the evaluation. Conversely, alternatives with lower priority values are ranked lower in the hierarchy. Additionally, Fig. 4 visually depicts the distribution of weights across the various alternatives. This graphical representation highlights that Alternative 3 possesses a greater weight compared to the other alternatives,

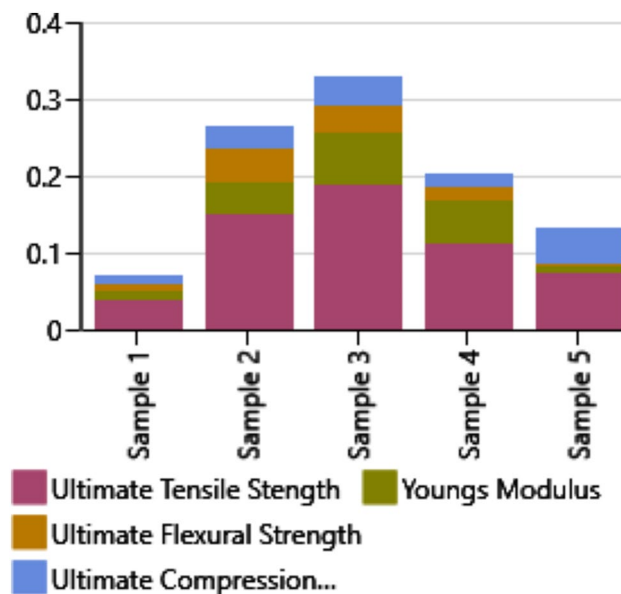


Fig. 5. Alternative weight distribution based each criteria.

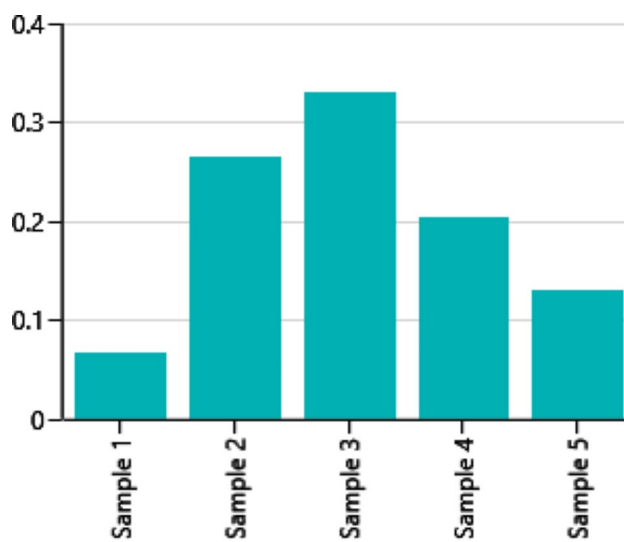


Fig. 6. Criteria weights on alternatives.

underscoring its relative importance and potential advantages in the decision-making process. By examining both the ranking table and the weight distribution, it becomes evident how effectively the alternatives were assessed, and it reinforces the selection of alternative 3 as a leading option based on its prioritized evaluation. This approach ensures a more informed decision-making process that accounts for multiple factors influencing the alternatives' performance. **Table 11**

Figure 5 presents a comprehensive overview of the criteria weights assigned to each alternative, highlighting the varying mechanical properties exhibited by each. Among these alternatives, Alternative 3 stands out for its superior performance in terms of Ultimate Tensile Strength (UTS), indicating its robust capacity to withstand tensile loads. This alternative demonstrates a notable advantage in strength, signifying its potential for applications requiring high tensile resilience.

In contrast, when evaluating Young's Modulus, Alternative 3 displays a moderate level of stiffness, suggesting that while it maintains a certain degree of rigidity, it may not be the most rigid option available. Additionally, the analysis reveals that Alternative 3 exhibits lower performance in terms of Ultimate Flexural Strength (UFS). This indicates that it may have limitations in resisting bending forces compared to other alternatives. Furthermore, the Ultimate Compressive Strength (UCS) of Alternative 3 is characterized as moderate, showcasing its ability to endure compressive loads but not as robustly as some of the other tested alternatives. Overall, Fig. 6 effectively captures the nuanced mechanical properties of Alternative 3, providing valuable insights into its strengths and

weaknesses across different criteria, which is essential for understanding its suitability for various engineering applications.

Figure 7 illustrates the ranking of various alternatives, highlighting that Alternative 3 stands out due to its superior mechanical properties. This assessment is based on critical criteria, including ultimate tensile strength (UTS), Young's modulus, ultimate flexural strength (UFS), and ultimate compressive strength (UCS). The comprehensive evaluation of these parameters demonstrates that Alternative 3 not only meets but exceeds the performance benchmarks established for the study. By analyzing UTS, we observe that Alternative 3 possesses exceptional resistance to tensile forces, while its Young's modulus indicates enhanced stiffness, suggesting that it can effectively withstand deformation under stress. Additionally, the ultimate flexural strength reflects its capacity to endure bending forces without failure, and the ultimate compressive strength indicates its durability under axial loads. Collectively, these results position Alternative 3 as the most robust alternative among the tested specimens, showcasing its potential for applications that demand high-performance materials in engineering and manufacturing contexts.

The rankings derived from the analyses exhibit remarkable stability, even when a higher priority is placed on tensile and flexural properties or when additional weight is assigned to tensile strength and compression metrics. This consistency underscores the robustness of the rankings established through the sensitivity analyses conducted. As depicted in Fig. 4, the sensitivity analysis for adjusting the weight of criteria C1 and C4 reveals that the rankings experience only slight modifications, indicating that the overall order remains largely unaffected by the shifts in emphasis.

Furthermore, the previously established parameters remain unchanged throughout these adjustments, reinforcing the reliability of the selected criteria and their associated weights in evaluating the performance characteristics of the materials. This level of consistency highlights the accuracy and validity of the decision-making process employed in this study, suggesting that the rankings are not only reliable but also resilient to variations in criteria prioritization.

Figure 8 illustrates the results of a sensitivity analysis that examines the effects of varying the weights assigned to criteria C1 and C2. This analysis reveals that making adjustments to these weights results in only slight shifts in the overall ranking of alternatives. Notably, despite these minor changes in ranking, the recommended parameters remain unchanged throughout the analysis. This indicates a level of robustness in the decision-making process, suggesting that the selected criteria and their assigned weights have a relatively stable influence on the outcomes. Such stability is critical in ensuring the reliability of the results and the consistency of the recommended parameters, reinforcing the validity of the methodology employed in this research. By confirming that the primary recommendations are unaffected by variations in weighting, the analysis demonstrates that the model maintains its integrity and can withstand fluctuations in criterion importance.

Figure 9 presents a detailed sensitivity analysis concerning the variation of weights assigned to criteria A1 and A5. This analysis reveals that modifying the weights results in moderate fluctuations in the overall ranking of alternatives. Despite these changes in ranking, it is noteworthy that the recommended parameters remain unchanged. This indicates a level of robustness in the decision-making process, suggesting that the selected parameters retain their validity and relevance even when the relative importance of specific criteria is altered. The findings from this sensitivity analysis underscore the stability of the proposed solutions, providing confidence that they will perform effectively under various weighting scenarios. Thus, while the rankings may experience some shifts, the core recommendations for the optimal parameters remain consistent, highlighting the effectiveness of the evaluation method used in this study.

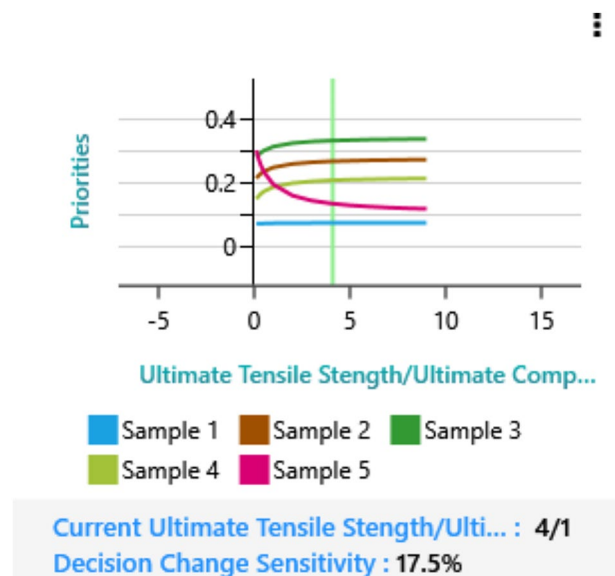


Fig. 7. Prioritizing of alternatives.

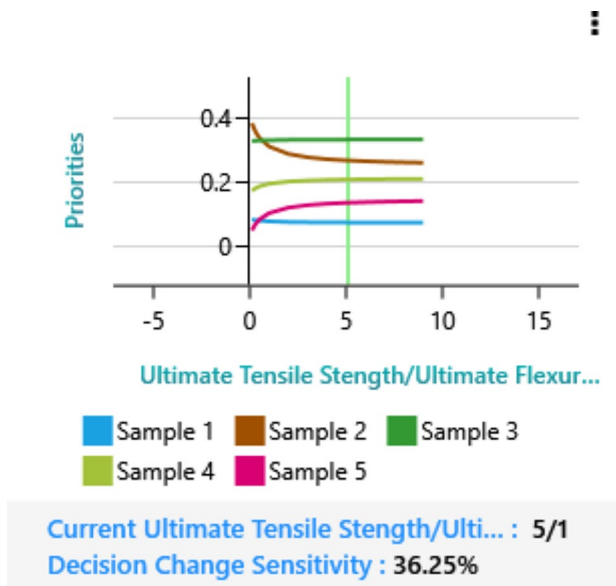
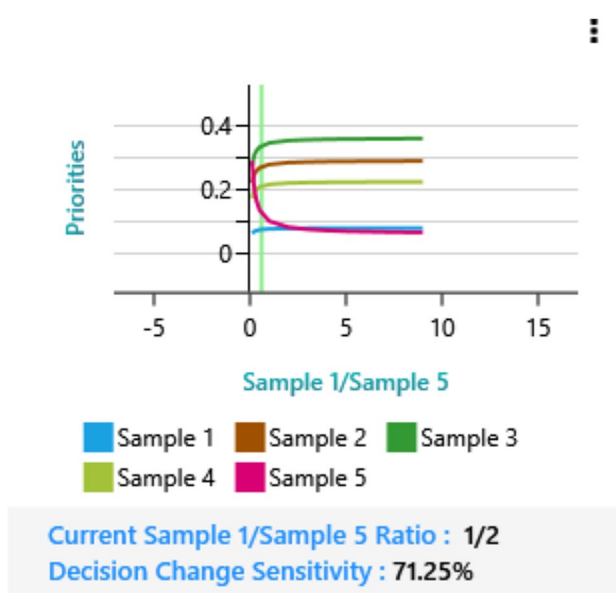
**Fig. 8.** Change the criteria weight of C1/C2.**Fig. 9.** Change the criteria weight of A1/A5.

Figure 10 illustrates the sensitivity analysis focusing on the adjustment of weights between criteria A1 and A2, which resulted in notable changes in the ranking order. Despite these shifts, the recommended process parameters remained consistent. Table 12 offers a comparison between rankings generated by the PSI Multi-Criteria Decision Making (MCDM) technique and those from the fuzzy AHP-TOPSIS rating method. In a study by Maniya and Bhatt³², the preference selection index method was applied to calculate the final preference score by assessing the preference values among various alternatives and their variations. This comparative analysis provided valuable insights into the differences observed in rankings produced by different MCDM techniques. Notably, the rankings derived from the various MCDM methods closely aligned with those produced by the Spice Logic AHP rating approach, demonstrating consistency in the selection process across methodologies. This consistency reinforces the reliability of the decision-making tools used in this study.

In this study, the selection of the data validation method depends on the specific criteria used. Previous researchers have mainly focused on the tensile and flexural properties when manufacturing impellers, considering them as crucial mechanical properties¹⁰. The comparison between the two studies reveals key insights into the effectiveness of different data validation and optimization methods used in additive manufacturing of G-PETG impellers. Both studies emphasize the importance of selecting appropriate process parameters based on previous

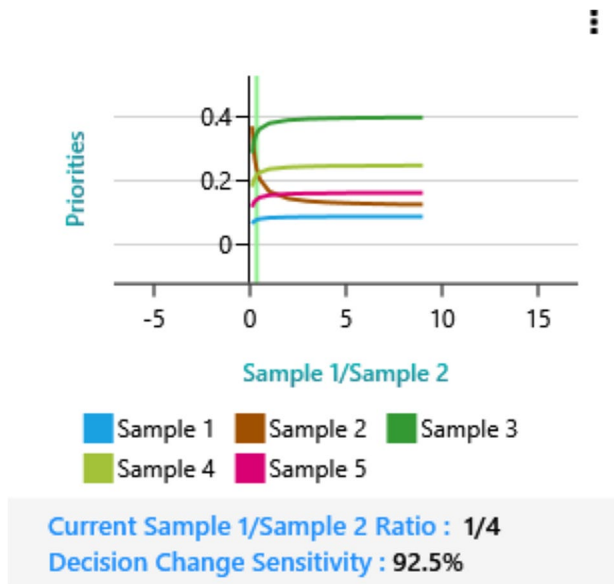


Fig. 10. Change the criteria weight of A1/A2.

Alternatives	Alternative 1	Alternative 2	Alternative 3	Alternative 4	Alternative 5
Preference Selection Index (PSI) Method	V	II	I	IV	III
Fuzzy-AHP TOPSIS	V	II	I	IV	III
Spice Logic AHP (This method)	V	II	I	IV	III

Table 12. Comparison with preference selection index method.

research to enhance mechanical properties such as tensile strength, flexural strength, and compressive strength. However, while both utilize MCDM tools, the first study relies solely on the Analytical Hierarchy Process (AHP) methodology by Spice Logic, which, despite having fewer procedures, effectively identifies optimal parameter settings for improving mechanical performance.

In contrast, the second study explores a more comprehensive approach, combining AHP with other MCDM techniques like TOPSIS and Fuzzy FAHP to address uncertainties and improve decision-making accuracy. This integrated approach offers a more nuanced evaluation of mechanical properties, demonstrating a greater adaptability to varying conditions in the manufacturing process. Expert validation plays a crucial role in both studies, ensuring that the optimization techniques applied are reliable and appropriate for achieving desired outcomes. Ultimately, while both studies successfully optimize mechanical properties, the second study's incorporation of multiple decision-making methods provides a more flexible and reliable framework for optimization, particularly in complex manufacturing environments. Figure 11 illustrates the decision process flowchart of this research.

This approach ensures the validity of the chosen criteria. Subsequently, the process parameters are selected based on those commonly used by previous researchers to ensure the selection of appropriate parameters in FDM printing, which in turn affects the mechanical properties. The optimization tool chosen for selection and optimization is highly suitable, although it involves slightly fewer procedures and is less reliable compared to other MCDM tools. Another noteworthy aspect is that the research model has been validated by experts in the field of MCDM. The results of the experiments provide valuable insights into the performance optimization of G-PETG impellers using the Analytical Hierarchy Process (AHP) methodology by Spice Logic. The ultimate tensile strength (UTS) data across different trials reveals notable variations in material performance. In Trial I, the average UTS ranged from 52.3 MPa to 63.4 MPa, while Trial III exhibited a wider range of 50.4 MPa to 69.1 MPa. This variation underscores the impact of additive manufacturing parameters on the mechanical properties of G-PETG. The AHP methodology effectively identified parameter settings that optimize UTS, highlighting the balance between achieving high strength and maintaining process consistency.

The Young's modulus measurements demonstrate a similar pattern, with Trial III achieving the highest average Young's modulus of 735.6 MPa. This indicates that under specific conditions, the G-PETG impellers exhibit enhanced stiffness, crucial for applications requiring rigidity. The AHP-based optimization approach enabled precise identification of parameters that improve material stiffness, confirming the robustness of the Spice Logic methodology in enhancing the mechanical properties of G-PETG.

In terms of ultimate flexural strength (UFS), the results range from 72 MPa to 89 MPa, reflecting the effect of various parameters on the material's resistance to bending forces. The average UFS values suggest that while

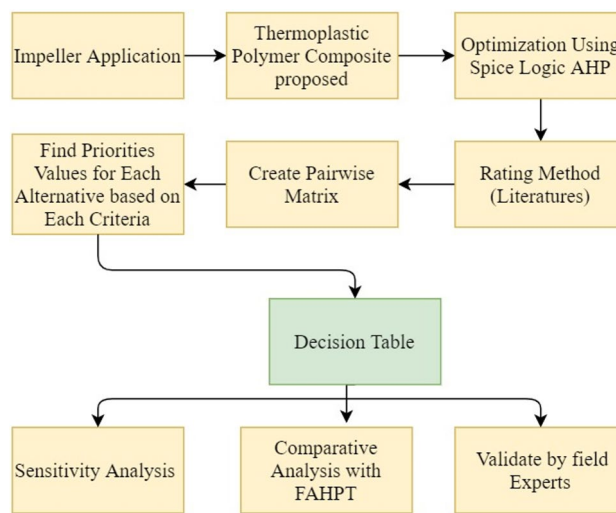


Fig. 11. Decision process flow chart.

some parameter sets improve resistance to deformation, others offer less benefit. The AHP methodology by Spice Logic was instrumental in selecting the optimal parameters that balance flexural strength with manufacturability.

For ultimate compressive strength (UCS), Trial C yielded the highest average UCS of 85.3 MPa. This result is significant for the durability of impeller components under compressive loads. The AHP methodology facilitated the identification of process parameters that maximize UCS, demonstrating its effectiveness in optimizing compressive strength for practical applications.

Overall, the application of the Analytical Hierarchy Process methodology by Spice Logic has proven effective in enhancing the mechanical properties of G-PETG impellers. The optimization process successfully identified parameter settings that improve strength, stiffness, and durability, contributing to the overall performance and reliability of the G-PETG impellers. This comprehensive approach underscores the value of AHP in achieving superior manufacturing outcome.

Conclusion

In this study, we explored the optimization of FDM parameters for Graphene-Reinforced Polyethylene Terephthalate Glycol (G-PETG) through a systematic Multi-Criteria Decision-Making (MCDM) approach. The state of the art in additive manufacturing emphasizes the increasing use of advanced composites and the importance of process parameter optimization to achieve superior mechanical properties. Key findings from our research include:

- The G-PETG composite exhibited significant improvements, with the highest ultimate tensile strength (UTS) reaching 69.1 MPa and an average Young's modulus of 735.6 MPa, confirming its potential for high-performance applications in various industries.
- The Analytical Hierarchy Process (AHP) effectively identified the optimal printing parameters, including an extruder temperature of 240 °C, a layer height of 0.20 mm, and an infill density of 65%, leading to enhanced mechanical performance in the fabricated components.
- A sensitivity analysis demonstrated that adjustments in criteria weights significantly impacted rankings; however, the suggested parameters remained unchanged.
- The rankings derived from various MCDM methodologies, including the Preference Selection Index (PSI) and fuzzy AHP-TOPSIS, closely aligned, indicating that the AHP approach employed in this study provided reliable and consistent results.

Overall, this research contributes to the current state of the art by combining advanced graphene-based materials with optimized FDM processes, showcasing their potential to enhance the performance and application range of additive manufacturing. The findings underscore the importance of systematic approaches in material selection and process optimization for the future of sustainable manufacturing practices.

Data availability

The data used to support the findings of this study are included in the article. Should further data or information be required, these are available from the corresponding author upon request.

Received: 16 August 2024; Accepted: 18 November 2024

Published online: 28 December 2024

References

1. Tuli, N. T., Khatun, S. & Rashid, A. B. Unlocking the future of precision manufacturing: A comprehensive exploration of 3D printing with fiber-reinforced composites in aerospace, automotive, medical, and consumer industries. *Helion*. (2024).
2. Nguyen, V. T. et al. WAAM technique: process parameters affecting the Mechanical Properties and microstructures of Low-Carbon Steel. *Metals* **13** (5), 873 (2023).
3. Subramani, R., Kalidass, A. K., Muneeswaran, M. D. & Lakshmi pathi, B. G. Effect of fused deposition modeling process parameter in influence of mechanical property of acrylonitrile butadiene styrene polymer. *Appl. Chem. Eng.*, 7(1). (2024).
4. da Cunha, R. B., Brito, L. B. Q., Agrawal, P., de Figueiredo Brito, G. & de Melo, T. J. A. 4D printing of shape memory polyethylene terephthalate glycol/thermoplastic polyurethane (PETG/TPU) blends. *J. Manuf. Process.* **119**, 596–608 (2024).
5. Raj, T., Tyagi, B., Jain, A., Sahai, A. & Sharma, R. S. Investigating the influence of annealing and nozzle diameter on tensile strength of polyethylene terephthalate glycol composites. *J. Thermoplast. Compos. Mater.*, 08927057241239001. (2024).
6. Deivasikamani, S. M. Enhancing mechanical characteristics of PETG Carbon Fiber Composite through various Shell thickness in FDM Processing. *Int. Res. J. Adv. Eng. Hub (IRJAEH)*. **2** (04), 706–714 (2024).
7. Patel, K. S., Shah, D. B., Joshi, S. J., Aldawood, F. K. & Kchaou, M. Effect of process parameters on the mechanical performance of FDM printed carbon fiber reinforced PETG. *J. Mater. Res. Technol.* **30**, 8006–8018 (2024).
8. Iacob, D. V., Zisopoul, D. G. & Minescu, M. Technical-economical study on the optimization of FDM parameters for the manufacture of PETG and ASA Parts. *Polymers* **16** (16), 2260 (2024).
9. Bedi, S. S. & Mallesha, V. Investigating tribological performance in 3D-printed PETG/graphene composites of varying composition. *J. Reinf. Plast. Compos.*, 07316844241274294. (2024).
10. Raja, S., Praveenkumar, V., Rusho, M. A. & Yishak, S. Optimizing Additive Manufacturing parameters for Graphene-Reinforced PETG Impeller production: a fuzzy AHP-TOPSIS Approach. *Results Eng.*, 103018. (2024).
11. Raja, S. & Rajan, A. J. *A Decision-Making Model for Selection of the Suitable FDM Machine Using Fuzzy TOPSIS*. 2022. (2022).
12. Subramani, R. et al. Selection and optimization of Carbon-Reinforced Polyether Ether Ketone process parameters in 3D Printing—A rotating component application. *Polymers* **16** (10), 1443 (2024).
13. Raja, S. et al. *Selection of Additive Manufacturing Machine Using Analytical Hierarchy Process*. 2022 (2022).
14. Wang, C. N., Yang, F. C., Vo, N. T. & Duong, C. T. Optimizing efficiency in BaaS marketplaces: a DEA-Grey Integration Approach. *IEEE Access*. (2024).
15. Subramani, R. et al. *A Recent Trend on Additive Manufacturing Sustainability with Supply Chain Management Concept, Multicriteria Decision Making Techniques*. 2022. (2022).
16. Rahman, M. S. Computational Fluid dynamics for Predicting and Controlling Fluid Flow in Industrial Equipment. *Eur. J. Adv. Eng. Technol.* **11** (9), 1–9 (2024).
17. Vo, T. M. N. Centrifugal pump design: An optimization. *The Eurasia Proceedings of Science Technology Engineering and Mathematics*, **17**, 136–151. (2022).
18. Joas, A. Study on composite impellers for hydrogen-based centrifugal compressors. (2024).
19. Chew, G. & Asokan, K. Case Study on Additive Manufacturing Metallic and Non-Metallic Pump Impellers for Corrosive Application. In *Asia Turbomachinery & Pump Symposium. 2022 Proceedings*. Turbomachinery Laboratory, Texas A&M Engineering Experiment Station (2024), February.
20. Hernandez-Carrillo, I., Wood, C. J. & Liu, H. Advanced materials for the impeller in an ORC radial microturbine. *Energy Procedia*. **129**, 1047–1054 (2017).
21. Polák, M. Behaviour of 3D printed impellers in performance tests of hydrodynamic pump. In Proceedings of the 7th International Conference on Trends in Agricultural Engineering, Prague, Czech Republic, 17–20 September ; pp. 17–20 (2019).
22. Tientcheu, S. W. T., Djouda, J. M., Bouaziz, M. A. & Lacazet dieu, E. A review on fused deposition modeling materials with analysis of key process parameters influence on mechanical properties. *Int. J. Adv. Manuf. Technol.* **130** (5), 2119–2158 (2024).
23. Pavlovic, A., Slijivic, M., Krajsnik, M., Ilic, J. & Anic, J. Polymers in Additive Manufacturing: the case of a Water Pump Impeller. *FME Trans.*, **45** (3). (2017).
24. Olaifya, N. G. et al. Viscoelastic and properties of Amphiphilic Chitin in Plasticised Polylactic Acid/Starch Biocomposite. *Polymers* **14** (11), 2268. <https://doi.org/10.3390/polym14112268> (2022).
25. Raja S. & John Rajan, A. Selection of Polymer Extrusion Parameters by Factorial Experimental design – a decision making model. *Scientia Iranica*. <https://doi.org/10.24200/sci.2023.60096.6591> (2023).
26. Sherugar, S., Birkett, M. & Blacklock, M. Characterisation of print path deviation in material extrusion. *Progress Additive Manuf.* **9** (4), 1049–1060 (2024).
27. Mustafa, M. A. et al. A Decision-Making Carbon Reinforced Material Selection Model for Composite Polymers in Pipeline Applications. *Advances in Polymer Technology*, 2023. (2023).
28. Raja, S. & John Rajan, A. Challenges and Opportunities in Additive Manufacturing Polymer Technology: A Review Based on Optimization Perspective. *Advances in Polymer Technology*, 2023. (2023).
29. Nguyen, V. T. T. & Vo, T. M. N. Using traditional design methods to enhance AI-driven decision making. *IGI Global* (2024).
30. Wang, C. N., Yang, F. C., Vo, T. M. N., Nguyen, V. T. T. & Singh, M. Enhancing efficiency and cost-effectiveness: a groundbreaking bi-algorithm MCDM approach. *Appl. Sci.* **13** (16), 9105 (2023).
31. Raja, S. & John Rajan, A. Challenges and Opportunities in Additive Manufacturing Polymer Technology: A Review Based on Optimization Perspective, *Advances in Polymer Technology*, vol. Article ID 8639185, 18 pages, 2023. (2023). <https://doi.org/10.1155/2023/8639185>
32. Maniya, K. D. & Bhatt, M. G. An alternative multiple attribute decision making methodology for solving optimal facility layout design selection problems. *Comput. Ind. Eng.* **61** (3), 542–549 (2011).

Acknowledgements

We would like to extend our special thanks to SpiceLogic Inc. for providing permission to use their free edition software and for allowing the use of the company's name in this research. Your support has been invaluable to the success of this work.

Author contributions

Conceptualization, R.S., MAR & SY.; Methodology, R.S. & VKS.; Software, R.S. & MJ.; Validation, R.S., MJ., MAR, JS & SY.; Investigation, R.S.; Resources, R.S.; Data curation, R.S.; Writing—original draft, R.S. & AKT.; Writing—review & editing, R.S. & AKT.; Visualization: MAR & SY.; Supervision, RS & JS.; Funding acquisition, MJ & MAR.

Funding statement

This work is partially funded by Centre for Sustainable Materials and Surface Metamorphosis. Chennai Institute of technology, India, vide funding number CIT/CSMSM/2024/RP/002.

Declarations

Competing interests

The authors declare no competing interests.

Additional information

Correspondence and requests for materials should be addressed to S.R. or S.Y.

Reprints and permissions information is available at www.nature.com/reprints.

Publisher's note Springer Nature remains neutral with regard to jurisdictional claims in published maps and institutional affiliations.

Open Access This article is licensed under a Creative Commons Attribution-NonCommercial-NoDerivatives 4.0 International License, which permits any non-commercial use, sharing, distribution and reproduction in any medium or format, as long as you give appropriate credit to the original author(s) and the source, provide a link to the Creative Commons licence, and indicate if you modified the licensed material. You do not have permission under this licence to share adapted material derived from this article or parts of it. The images or other third party material in this article are included in the article's Creative Commons licence, unless indicated otherwise in a credit line to the material. If material is not included in the article's Creative Commons licence and your intended use is not permitted by statutory regulation or exceeds the permitted use, you will need to obtain permission directly from the copyright holder. To view a copy of this licence, visit <http://creativecommons.org/licenses/by-nc-nd/4.0/>.

© The Author(s) 2024